Appl. Phys. B (2016) 122:40
DOI 10.1007/s00340-016-6321-3

Applied Physics B
Lasers and Optics

Extended emission wavelength of random dye lasers by exploiting radiative and non-radiative energy transfer

Wan Zakiah Wan Ismail[1,2,3] · **Ewa M. Goldys**[1] · **Judith M. Dawes**[1,2]

Received: 19 August 2015 / Accepted: 4 January 2016 / Published online: 19 February 2016
© Springer-Verlag Berlin Heidelberg 2016

Abstract We demonstrate long-wavelength operation (>700 nm) of random dye lasers (using a methylene blue dye) with the addition of rhodamine 6G and titania, enabled by radiative and non-radiative energy transfer. The pump energy is efficiently absorbed and transferred to the acceptors, to support lasing in random dye lasers in the near infrared. The optimum random laser performance with the highest emission intensity and the lowest lasing threshold was achieved for a concentration of methylene blue as the acceptor equal to 6× the concentration of rhodamine 6G (donor). Excessive levels of methylene blue increased the lasing threshold and broadened the methylene blue emission linewidth due to dye quenching from re-absorption. This is due to competition between the donor emission and energy transfer and between absorption loss and fluorescence quenching. The radiative and non-radiative energy transfer is analyzed as a function of the acceptor concentration and pump energy density, with consideration of the spectral overlap. The dependence of the radiative and non-radiative transfer efficiency on the acceptor concentration is obtained, and the energy transfer parameters, including the radiative and non-radiative energy transfer rate constants (K_R and K_{NR}), are investigated using Stern–Volmer analysis. The analysis indicates that radiative energy transfer is the dominant energy transfer mechanism in this system.

1 Introduction

Research into random dye lasers has grown rapidly since the earliest report in 1966 [1]. Random dye lasers include scatterers to scatter light and a dye medium for light amplification. These lasers have applications in sensing and imaging [2–4]. Random dye lasers based on materials such as dielectrics, metals, polymers and liquid crystals have been reported [5–14]. Organic dyes such as rhodamine are commonly used in random lasers due to their broad absorption spectra, high gain and compatibility with available pump wavelengths (such as 532 nm), while methylene blue, oxazine and nile blue dyes are not compatible with blue and green pump light. We combine these dyes in a single laser to extend the random laser emission to near infrared wavelengths through the process of energy transfer.

The energy transfer (redistribution of excitation energy between a short-wavelength dye, donor and a long-wavelength acceptor) is either radiative, where the donor molecule emits a photon which is subsequently absorbed by the acceptor molecule, or non-radiative, where the excited donor transfers its excitation energy to a ground-state acceptor through a radiationless/non-radiative process. Non-radiative energy transfer is also known as Forster (fluorescence) resonance energy transfer (FRET) [15–17]. For both radiative and non-radiative energy transfer, a significant overlap of the donor emission spectrum and the

Electronic supplementary material The online version of this article (doi:10.1007/s00340-016-6321-3) contains supplementary material, which is available to authorized users.

✉ Wan Zakiah Wan Ismail
wan-zakiah-binti.wan-ismail@students.mq.edu.au

[1] Department of Physics and Astronomy, MQ Photonics Research Centre, Macquarie University, Sydney, NSW 2109, Australia

[2] ARC Centre of Excellence for Ultrahigh Bandwidth Devices for Optical Systems (CUDOS), Sydney, Australia

[3] Faculty of Science and Technology, Islamic Science University of Malaysia, 71800 Nilai, Negeri Sembilan, Malaysia

acceptor absorption spectrum is required to support long-range multipole interactions [15–17].

Energy transfer-based random lasing was introduced previously in Refs. [18–21]. Shi et al. [18] demonstrated cascaded radiative energy transfer between three different dyes in separate cuvettes. Luis et al. [19] and Alee et al. [20] studied FRET random lasers using mixtures of rhodamine 6G/Nile blue and coumarin/rhodamine 6G, respectively. Luis et al. [19] observed laser emission from a mirror cavity within the sample cell, and Alee et al. [20] observed the enhancement of a FRET random laser by varying the concentration of scatterers. Lopez et al. [21] studied FRET random lasing by doping a DNA-lipid complex with two different dyes and tuning the emission wavelength by varying sphere diameters. They observed a narrow emission peak (~15 nm) at ~700 nm at the acceptor wavelength.

Here, we report the following observations: (1) random dye laser emission in the near infrared (>700 nm) with a narrow emission linewidth (~4 nm), ~3× narrower than reported in [21]. This was achieved in a random dye laser system incorporating rhodamine 6G (Rh6G)/methylene blue (MB)/titania pumped with 532-nm light. We attribute this infrared emission to energy transfer between Rh6G and methylene blue dye molecules. (2) We found that energy transfer influences the random lasing threshold, shifts the emission peak wavelength and changes the emission linewidth, depending on the dye concentration ratio. The optimum MB concentration was identified for a Rh6G concentration of 5×10^{-4} M. (3) We analyzed energy transfer based on the radiative, dipole–dipole energy transfer and Stern–Volmer expressions, taking into account the acceptor concentration and energy density of the pump laser. Our theoretical analysis indicates that the radiative energy transfer efficiency dominates the non-radiative energy transfer efficiency for all acceptor concentrations. We aim to analyze the influence of energy transfer in random dye lasers, and this approach provides an alternative to analyze FRET by using technically more challenging fluorescence lifetime measurements.

2 Theoretical considerations

The radiative and non-radiative energy transfer in the system under consideration is analyzed using rate equations combined with Stern–Volmer plots. This allows us to estimate the radiative (K_R) and non-radiative (K_{NR}) rate constants. The rate equations of the donor–acceptor dye mixture at the lasing threshold are [15]:

$$\frac{dN_{1D}}{dt} = N_{0D}\sigma_D W(t) - K_{NR}N_{1D}N_{0A} - \frac{N_{1D}}{\tau_D} \quad (1)$$

$$\frac{dN_{1A}}{dt} = N_{0A}\sigma_A W(t) + (K_{NR} + K_R)N_{1D}N_{0A} - \frac{N_{1A}}{\tau_A} \quad (2)$$

$$N_D = N_{0D} + N_{1D}$$

$$N_A = N_{0A} + N_{1A}$$

where N_{0D}, N_{1D}, N_{0A} and N_{1A} are the population densities of donor (D) and acceptor (A) molecules in the ground (0) and excited (1) states, respectively. σ_D and σ_A are the absorption cross sections for donors and acceptors at the pump wavelength (532 nm), τ_D and τ_A are the fluorescence lifetimes of the donor and acceptor without energy transfer, respectively, and $W(t)$ is the pump rate. Figure S1 illustrates the above scheme (Supporting information).

Dipole–dipole, dipole–quadrupole and quadrupole–quadrupole interactions among dye molecules contribute to non-radiative energy transfer. Here, we assume only dipole–dipole interactions. An oscillating dipole is generated when a fluorescent 'donor' probe is excited to resonate with a dipole of an 'acceptor' probe in the near field. The emission of the Rh6G fluorophores (donor) can couple to the excitation of the MB fluorophores (acceptor) when the acceptor dipole interacts with the donor dipole through non-radiative energy transfer [16]. The non-radiative energy transfer efficiency is given by [15, 22],

$$\eta_{NR} = \pi^{1/2} X \exp\left(X^2\right)(1 - \mathrm{erf}(X)) \quad (3)$$

where X is the ratio of molar acceptor concentration $[A]$ to the critical molar acceptor concentration $[A]_o$ as defined below:($X = [A]/[A]_o$). The function erf (X) is given by:

$$\mathrm{erf}(X) = \frac{2}{\pi^{1/2}} \int_0^X \exp\left(-t^2\right) dt \quad (4)$$

and $[A]_o$ is [22]:

$$[A]_o = \frac{3000}{2\pi^{\frac{3}{2}} N (R_0)^3} \quad (5)$$

where N is Avogadro's number and R_o is the critical transfer distance of donor and acceptor molecules. R_o is given by [15, 23]:

$$R_o = \left(\frac{3000}{4\pi N [A]_{1/2}}\right)^{1/3} = \frac{7.35}{\left([A]_{1/2}\right)^{1/3}} \text{ (in Angstroms, Å)} \quad (6)$$

where $[A]_{1/2}$ is the half-quenching concentration which can be obtained under the condition [15]:

$$I_{DA} = I_D/2 \quad (7)$$

where I_{DA} and I_D are the emission intensities of the donor in the presence and absence of the acceptor, respectively. According to the Forster energy transfer theory, R_o (the

Forster distance) is related to the energy transfer probability (rate), P_{DA} as [15]:

$$P_{DA} = \frac{1}{\tau_D}\left(\frac{R_0}{R}\right)^s \tag{8}$$

where s is 6 for dipole–dipole, 8 for dipole–quadrupole and 10 for quadrupole–quadrupole interactions, τ_D is the fluorescence lifetime of the donor molecules without acceptors, and R is the average distance between the donor and acceptor.

The radiative energy transfer efficiency (η_R) is obtained from the total energy transfer efficiency, η_T [15]:

$$\eta_T = \eta_R + \eta_{NR} \tag{9}$$

where

$$\eta_R = 1 - \frac{I_{DA}}{I_D} \tag{10}$$

$$\eta_{NR} = 1 - \frac{\varphi_{DA}}{\varphi_D} \tag{11}$$

where φ_{DA} and φ_D are the quantum yields with and without acceptors.

The radiative and non-radiative rate constants can be determined from Stern–Volmer plots, as shown by [15, 24]:

$$\frac{I_D}{I_{DA}} = 1 + K_T \tau_D [A] \tag{12}$$

$$\frac{\varphi_D}{\varphi_{DA}} = 1 + K_{NR} \tau_D [A] \tag{13}$$

where K_T and K_{NR} are the total and non-radiative rate constants and $[A]$ is the concentration of acceptors.

3 Method

3.1 Sample preparation

Methanol solutions with Rh6G (fixed concentration, 5×10^{-4} M) and MB (various concentrations, 1×10^{-4}–9×10^{-3} M; Sigma-Aldrich) in dye ratios ranging from 1:1 to 1:18 were added to titania nanoparticles (200 nm particle diameter, number density 1×10^{11} cm^{-3}) (Sigma-Aldrich), and the solutions were placed in a cuvette (1 cm × 1 cm). Gain is provided by both dyes, while titania exhibits scattering effects due to its large refractive index contrast with the solvent, methanol (titania, 2.6 and methanol, 1.33). The transport mean free path, l_t, of the solution of titania nanoparticles without dyes, ~242 μm, was estimated from a coherent backscattering (CBS) experiment [25, 26]. The systems operated in the diffusive regimes under the condition: the emission light wavelength, $\lambda < l_t < L$ [27].

3.2 Optics experiments

The absorption and fluorescence spectra were measured using a Cary spectrophotometer (Varian Australia) and Fluorolog (Horiba Jobin Yvon) spectrofluorometer. For random laser measurements, the samples were excited with a Q-switched, frequency-doubled Nd:YAG laser (532 nm, 10 Hz, 4 ns) with a 3-mm-diameter excitation spot size at the sample (L) at an angle of 45° to the normal to the front face of the cuvette, and the emission light was collected from the front face of the cuvette at 30° to the normal by a lens ($f = 5$ cm) and measured by a fiber-coupled spectrometer (Ocean Optics spectrometer with a resolution ~1 nm). A thin Teflon sheet inside the cuvette prevented back-reflection from the cuvette's faces, and a 532-nm edge filter blocked residual pump light from the spectrometer.

4 Experimental and theoretical results

4.1 Absorption and fluorescence spectra of donors and acceptors

The fluorescence and absorption spectra for both dyes are plotted in Fig. 1 (Rh6G and MB). This shows the spectral overlap between the donor fluorescence spectrum (Rh6G) and the acceptor absorption spectrum (MB) and indicates the possibility of energy transfer between these two dye molecules.

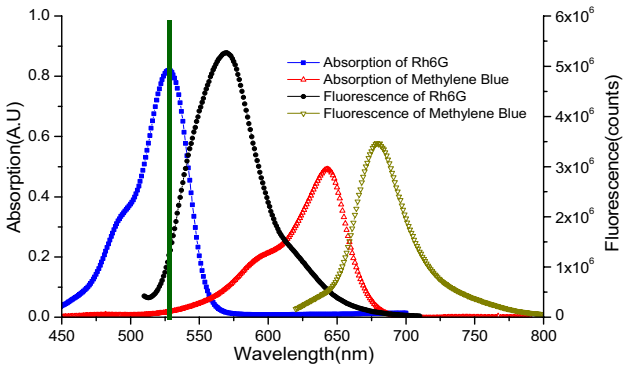

Fig. 1 Absorption spectra of Rh6G (*blue curve*) and MB (*red curve*); fluorescence spectra of Rh6G (*black curve*) and MB (*olive curve*). Both dyes have the same concentration, 5×10^{-4} M. The *green line* shows the laser excitation at λ ~ 532 nm

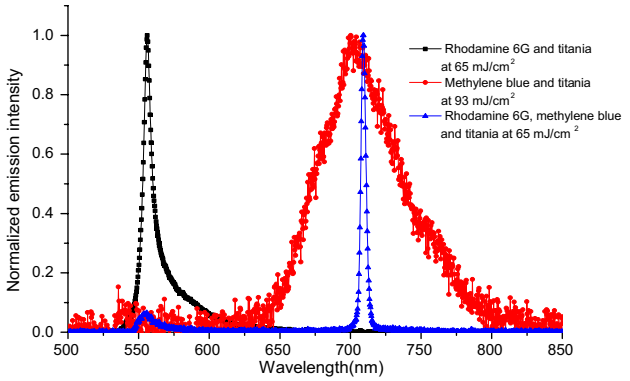

Fig. 2 Emission spectra of Rh6G/titania, MB/titania and Rh6G/titania/MB random lasers. A Rh6G (5×10^{-4} M)/titania (1×10^{11} cm^{-3}) random laser is shown by the *black curve*. A MB (3×10^{-3} M)/titania (1×10^{11} cm^{-3}) random laser excited at 93 mJ/cm^2 is shown by the *red curve*. The emission from the Rh6G (5×10^{-4} M)/titania (1×10^{11} cm^{-3})/MB (3×10^{-3} M) random laser is shown by the *blue curve*

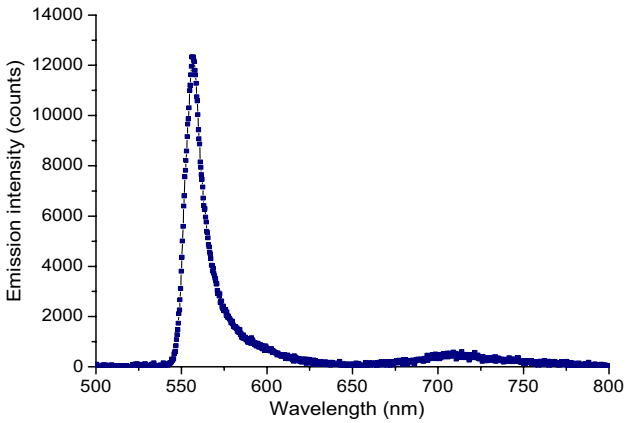

Fig. 3 Emission spectra of Rh6G (5×10^{-4} M)/MB (5×10^{-4} M)/titania (1×10^{11} cm^{-3}) random lasers, excited at ~42 mJ/cm^2

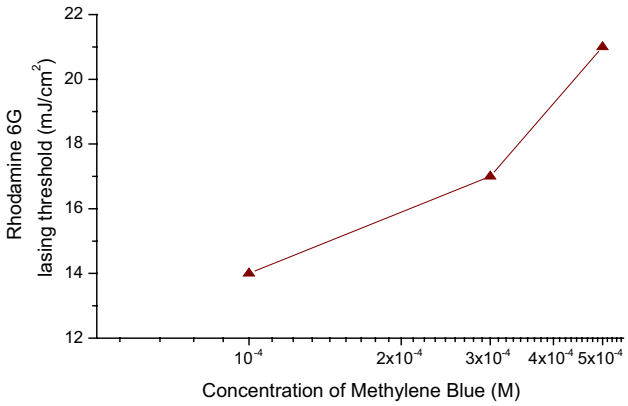

Fig. 4 Comparison of Rh6G threshold of Rh6G/titania/MB random lasers for low concentrations of MB (1×10^{-4}–5×10^{-4} M). The concentration of Rh6G is fixed at 5×10^{-4} M

4.2 Spectral narrowing for random lasers based on dielectric nanoparticles

Due to the inefficient pump absorption of MB (see green line in Fig. 1), a random laser with MB and titania nanoparticles, pumped at 93 mJ/cm^2, does not reach lasing threshold. No spectral narrowing is observed in the MB/titania emission (Fig. 2). However, the addition of Rh6G allows this system to lase at ~710 nm with a low threshold.

Below the lasing threshold (figure S2 in Supporting information), the (Rh6G) emission intensity peaks at ~560 nm with no lasing emission at ~710 nm, but when the system reaches threshold, it emits at ~710 nm (MB), with reduced Rh6G fluorescence.

4.3 Rhodamine 6G emissions of rhodamine 6G/methylene blue/titania random lasers for low concentrations of MB (1×10^{-4} to 5×10^{-4} M)

For Rh6G/MB titania random lasers with low MB concentrations (1×10^{-4}–5×10^{-4} M), a narrow emission peak appears at ~560 nm instead of ~710 nm. Figure 3 shows the emission spectra of Rh6G (5×10^{-4} M)/MB (5×10^{-4} M)/titania (1×10^{11} cm^{-3}) random lasers, excited at ~42 mJ/cm^2. The emission intensity of Rh6G decreases (figure S3 in Supporting information) and the Rh6G lasing threshold increases (Fig. 4) when the MB concentration is increased from 1×10^{-4} to 5×10^{-4} M. This is attributed to the energy transfer from Rh6G to MB. Rh6G affects not only the MB emission but also its lasing threshold. For MB concentrations from 1×10^{-4} to 5×10^{-4} M, Rh6G lasing is observed, but no MB emissions are observed (figures S3 in supporting information). At these low MB concentrations, there is insufficient gain for MB, resulting in lasing at ~560 nm.

4.4 Methylene blue and rhodamine 6G emissions of rhodamine 6G/methylene blue/titania random lasers for increased concentrations of MB (1×10^{-3}–9×10^{-3} M)

Increasing the MB concentration to 1×10^{-3} M produces lasing with a narrow emission peak at ~710 nm (Fig. 5) because the energy is efficiently transferred from the donor (Rh6G) to the acceptor (MB). For a MB concentration of 3×10^{-3} M, the emission spectrum at ~560 nm substantially reduces (4× lower than that for 1 mM concentration MB) because the energy absorbed by the Rh6G dye is mostly transferred to the MB. Adding more MB broadens the emission at ~710 nm (Fig. 5c–e). The MB emission spectrum for MB concentration above 12× Rh6G is broad

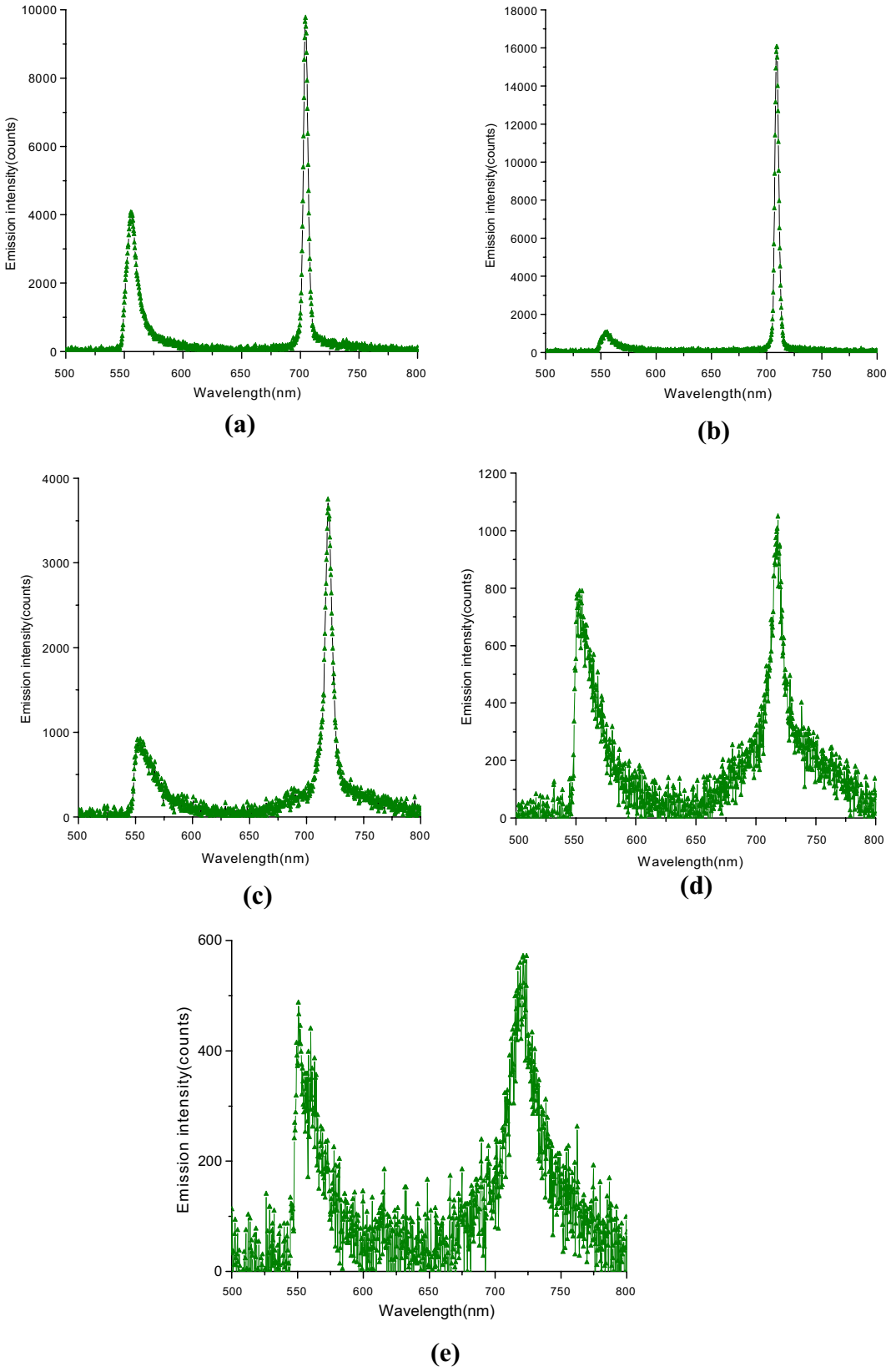

Fig. 5 Emission spectra of Rh6G/MB/titania random lasers with fixed donor concentration (5×10^{-4} M) and varied acceptor concentrations; **a** 1×10^{-3} M, **b** 3×10^{-3} M, **c** 4×10^{-3} M, **d** 5×10^{-3} M and **e** 6×10^{-3} M. All samples are excited at ~65 mJ/cm^2

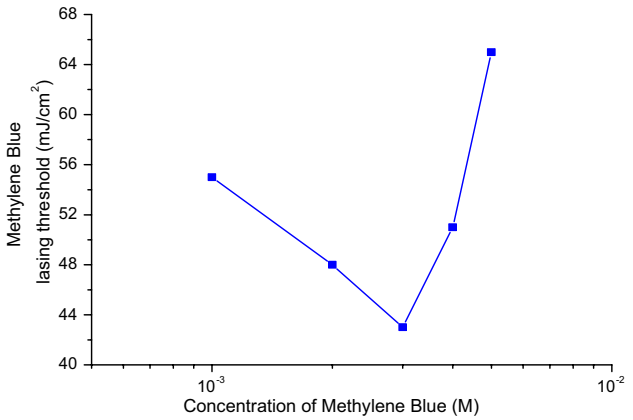

Fig. 6 Lasing thresholds of Rh6G/titania/MB random lasers (~710 nm emission) for increased MB concentrations (1×10^{-3}–5×10^{-3} M). The concentration of Rh6G is fixed at 5×10^{-4} M

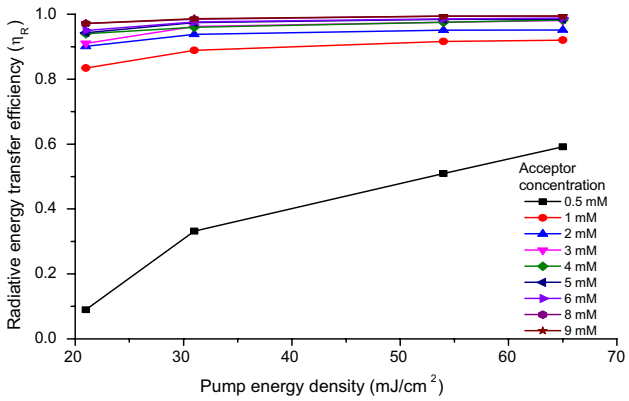

Fig. 7 Estimated radiative energy transfer rate (η_R) for various acceptor concentrations in Rh6G/MB/titania random lasers based on different pump energy density

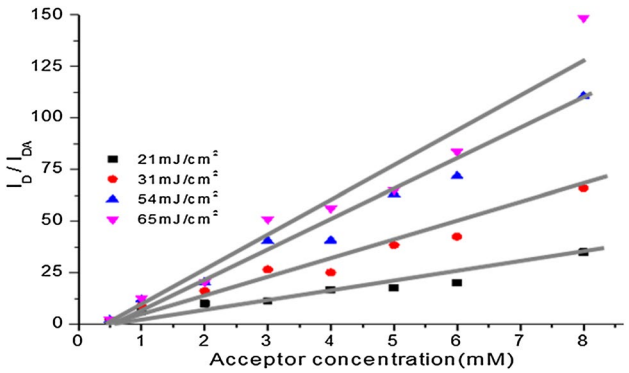

Fig. 8 I_D/I_{DA} for various acceptor concentrations for different pump energy densities. The *gray lines* are fitted to the data

even for the highest pump energy density, indicating no lasing is achieved (figure S4 in supporting information).

When the MB concentrations increase from 1×10^{-3} to 5×10^{-3} M, we observe MB lasing (figure S5 in supporting information). Lasing thresholds for MB emission are clearly observed when the emission peak intensity increases nonlinearly with the pump energy density. The Rh6G emission intensity shows a linear increase with the pump energy density compared with the MB emission intensity, so no lasing threshold for Rh6G emission. The lasing thresholds of MB emission for different concentrations of MB are evident in Fig. 6 where 3 mM of MB achieves the lowest lasing threshold in the present system. No lasing is observed for MB concentrations above 12× Rh6G (figure S7, supporting information).

MB has a fluorescence quantum yield of 4 % in water and a high proportion of dimer (with a characteristic absorption peak, λ_{abs} ~590 nm) [28] as shown in Fig. 1. In contrast, the Rh6G quantum yield is substantially higher (95 % [29]). We find that the optimum MB concentration for our near infrared random dye lasers should be 6× greater than that of Rh6G (3 mM MB concentration). At 3 mM MB concentration, we obtained the lowest lasing threshold with the highest MB emission peak intensity. The corresponding slope of the threshold curves for 3 mM concentration MB is 1.3× and 3× higher than that for 2 and 4 mM concentration MB, respectively (figures S5 and S6 in Supporting information).

4.5 Theoretical analysis

In this study, the theoretical analysis is done for MB concentrations from 5×10^{-4} to 5×10^{-3} M. The η_{NR} is calculated from Eq. (3) with $[A_0]$ being estimated as 0.56 M. The η_{NR} increases linearly from 0.002 to 0.02 for MB concentrations 5×10^{-4}–5×10^{-3} M. The radiative energy transfer efficiency, η_R, versus pump energy density is shown in Fig. 7; here, η_R increases with acceptor concentration. Figure 7 shows that η_R is reduced for low MB concentration (5×10^{-4} M) compared with higher MB concentrations because there is no lasing emission at the acceptor wavelength (see Fig. 3). When the MB concentration is increased, the radiative energy transfer efficiency approaches 1 following the appearance of emission peaks at ~710 nm (see Fig. 5). This shows that radiative energy transfer plays a crucial role in supporting lasing emission at the acceptor wavelength.

Kumar et al. [15] reported energy transfer from donors to acceptors for the situation when the concentration of donor ≥ concentration of acceptor and they observed negative slopes of η_R as a function of pump energy density. In the present system, we observe positive slopes of η_R as a function of pump energy density because the system operates in a different regime (concentration of

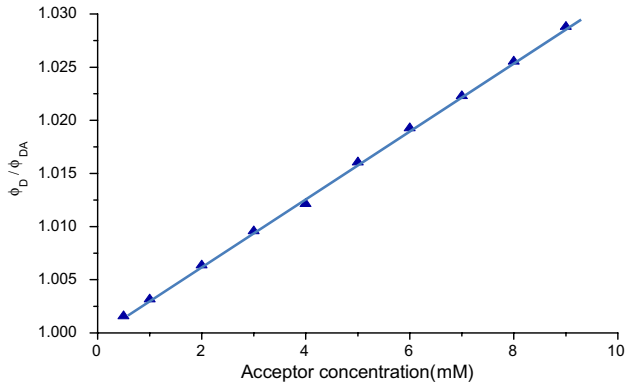

Fig. 9 Calculated φ_D/φ_{DA} versus various acceptor concentrations at 65 mJ/cm^2. The *blue line* is fitted to the data indicating a linear increase

donor ≤ concentration of acceptor). The positive slope arises because of the increased efficiency of energy transfer as a function of pump excitation since every pump photon can excite donor molecules which readily transfer the energy to an adjacent dye acceptor.

Stern–Volmer plots (Figs. 8, 9) are used to analyze the energy transfer in this system by calculating radiative and non-radiative rate constants in order to estimate the photophysical intermolecular deactivation process (fluorescence quenching) [15, 24]. Here, the fluorescence lifetime of the donor molecules without acceptors, τ_D, is ~4 ns [30].

Both ratios I_D/I_{DA} and φ_D/φ_{DA} are linearly proportional to the acceptor concentration, consistent with the Stern–Volmer expressions (Eqs. 12, 13). K_T and K_{NR} values can be found from the gradient, while K_R can be calculated from $K_T = K_R + K_{NR}$. Here, K_{NR} is estimated as 3×10^{10} M^{-1} s^{-1} and K_R ranges from 7×10^{11} to 4×10^{12} M^{-1} s^{-1} where τ_D is ~4 ns.

5 Discussion

We analyze the radiative and non-radiative energy transfer in this random laser due to the overlap of the donor fluorescence spectrum with the absorption spectrum of the acceptor, MB.

5.1 Experiment and theoretical analysis

The energy transfer from Rh6G dye molecules (donor) to MB dye molecules (acceptor) can be described by both radiative and non-radiative processes evaluated from the rate equations and the Stern–Volmer plots. The optimum random laser performance is observed at an acceptor concentration of 3 mM. We calculate the radiative energy transfer efficiency to be almost ~1, while the non-radiative energy transfer efficiency is much less. From the Stern–Volmer plots, the radiative energy transfer rate constant K_R (7×10^{11} to 4×10^{12} M^{-1} s^{-1}) is ~20× higher than K_{NR} (3×10^{10} M^{-1} s^{-1}) for all measured pump levels, showing that radiative energy transfer dominates the energy transfer from Rh6G to MB dye molecules.

5.2 FRET contribution in Rh6G/MB random lasers

Rh6G/MB/titania random lasers offer the probability of laser emission in both Rh6G and MB wavelength ranges. Because the Rh6G is a very efficient fluorescence emitter, it may lase over a wide range of conditions and transfer energy both radiatively and non-radiatively to MB which is a less efficient emitter.

We find at low MB concentrations (1×10^{-4}–5×10^{-4} M), Rh6G lases and shows evidence of non-radiative energy transfer (with decreased Rh6G emission peak intensity and increased Rh6G threshold as a function of increased MB concentration) [21].

As the MB concentration is increased (1×10^{-3}–5×10^{-3} M), lasing occurs at the MB emission since every pump photon contributes to more excitation. Laser emission develops at the MB emission peak and may compete with Rh6G for the available gain. At these MB/Rh6G concentration ratios, radiative energy transfer appears to dominate over non-radiative energy transfer as demonstrated by the radiative energy transfer efficiency for a concentration ≥1 mM (Fig. 7). In a mixture of two laser dyes, the Forster energy transfer occurs efficiently if the distance between the donor and acceptor is small <30 Å [31]. We estimate the average intermolecular spacing ($\frac{1}{\sqrt[3]{N_T}}$, [20]) is ~80 Å where N_T(total donor and acceptor molecules) ~2.1×10^{18} molecules/cm^3 when the MB concentration is 6× greater than the Rh6G concentration. At these concentrations, FRET may not be efficient for energy transfer. We note that it is challenging to create random lasers relying on the FRET mechanism with this pair of dyes due to their disparate fluorescence quantum yields.

5.3 Effects of energy transfer on emission intensity, emission linewidth and emission peak wavelength

Energy transfer affects the emission intensity of both donor (Rh6G) and acceptor (MB) (Figs. 3, 5) since the emission intensity varies based on increasing MB concentrations. The emission intensity is quantitatively related to the radiative and non-radiative transfer efficiency. At 5×10^{-4} M of MB concentration in Rh6G/MB/titania random lasers, the energy is not efficiently transferred from the donor to the acceptor as emission occurs at the Rh6G emission wavelength, but not at the MB emission wavelength. At this MB concentration, the radiative and non-radiative energy

transfer efficiencies are small (η_R ~0.6 and η_{NR} ~0.002). When more acceptor molecules (~3 mM of acceptor concentration) are added, the radiative and non-radiative energy transfer rates increase, leading to higher emission intensity at the MB wavelength (16× higher at ~65 mJ/cm^2) and reduced emission intensity at the Rh6G wavelength (12× lower at ~42 mJ/cm^2) than 0.5 mM of acceptor concentration (Figs. 3, 5). The emission intensity at the MB emission wavelength reaches the maximum value when most of the absorbed photons are re-emitted (see Fig. 5b). With the increased MB concentration (4 mM), the MB emission intensity reduces 4× (Fig. 5) than that for 3 mM MB concentration due to self-quenching acceptor–acceptor interactions due to re-absorption processes. Self-quenching arises with the increase in the non-radiative energy transfer efficiency [15]. Dye quenching not only decreases the emission intensity but also broadens the emission linewidth (Fig. 5).

The MB emission peak wavelength is red-shifted by about ~20 nm (from 1×10^{-3} to 6×10^{-3} M) at higher MB concentrations, due to self-absorption of MB leading to red-shifted emission (Fig. 5). The intermolecular separation between Rh6G and the MB molecules reduces with increasing MB concentration.

5.4 Effect of energy transfer on lasing threshold

Radiative and non-radiative energy transfer also significantly influences the Rh6G/MB/titania random laser threshold. Higher non-radiative energy transfer leads to losses when the energy is released in the form of heat rather than light.

When Rh6G dye molecules are not effectively pumping MB molecules, the lasing occurs at the Rh6G emission wavelength (Figs. 3, 4). As the MB concentration increases, the MB molecules absorb Rh6G emission more effectively, resulting in sufficient gain for the MB to lase. Increasing acceptor concentration provides more gain for lasing, with a reduced lasing threshold (55 mJ/cm^2 for 1 mM of MB concentration to 43 mJ/cm^2 for 3 mM of MB concentration). However, excess acceptor molecules experience self-quenching, which increases the lasing threshold (Fig. 6) or prevents lasing at the acceptor wavelength. Excess MB may also hinder efficient pump absorption by Rh6G, thus resulting in a higher lasing threshold.

6 Conclusions

Random lasing emission with a narrow emission peak (~4 nm) beyond 700 nm is achieved by combining two dyes with scatterers. Methylene blue (MB) dye is a less efficient dye for random lasers excited with 532 nm green light, but with the addition of rhodamine 6G (Rh6G), MB can reach the laser threshold. For low MB concentrations (1×10^{-4}–5×10^{-4} M), the random laser emission is from Rh6G at ~560 nm, whereas for MB concentrations (1×10^{-3}–5×10^{-3} M), the emission is from MB at ~710 nm. Both random laser emissions are affected by radiative and non-radiative energy transfer. The MB lasing emission intensity at ~710 nm is enhanced as the Rh6G emission intensity at ~560 nm reduces for MB concentrations from 1×10^{-3} to 5×10^{-3} M. A MB concentration (3×10^{-3} M) at 6× the Rh6G concentration is needed to achieve optimum random lasing. The radiative and non-radiative energy transfer efficiencies are compared using Stern–Volmer plots. Both radiative and non-radiative energy transfers influence the lasing threshold and spectral emission of random lasers depending on the acceptor concentration. Radiative energy transfer dominates in the present systems since K_R is 20 times higher than K_{NR}. Adding acceptors to facilitate energy transfer can improve the efficiency of random dye lasers, but an excess concentration of acceptors leads to fluorescence quenching.

Acknowledgments We acknowledge funding and support from the ARC Centre of Excellence Program, Centre for Ultrahigh-bandwidth Devices for Optical Systems, ARC DP140104458, an Australia Endeavour Award, and Macquarie University.

References

1. R.V. Ambartsumyan, N.G. Basov, P.G. Kryukov, V.S. Letokhov, A laser with a nonresonant feedback. IEEE J. Quantum Electron. **QE-2**, 442–446 (1966)
2. D.S. Wiersma, The physics and applications of random lasers. Nat. Phys. **4**, 359–367 (2008)
3. H. Cao, Random lasers: development, features and applications. Opt. Photonics News **16**, 24–29 (2005)
4. W.Z.W. Ismail, L. Guozhen, K. Zhang, E.M. Goldys, J.M. Dawes, Dopamine sensing and measurement using threshold and spectral measurements in random lasers. Opt. Express **24**, A85–A91 (2015)
5. J. Kitur, G. Zhu, M. Bahoura, M.A. Noginov, Dependence of the random laser behavior on the concentrations of dye and scatterers. J. Opt. **12**, 024009 (2010)
6. W.Z.W. Ismail, D. Liu, S. Clement, D. Coutts, E. Goldys, J. Dawes, Spectral and coherence signatures of threshold in random lasers. J. Opt. **16**, 105008 (2014)
7. Z. Wang, X. Shi, S. Wei, Y. Sun, Y. Wang, J. Zhou, J. Shi, D. Liu, Two-threshold silver nanowire-based random laser with different dye concentrations. Laser Phys. Lett. **11**, 095002 (2014)
8. L. Yang, G. Feng, J. Yi, K. Yao, G. Deng, S. Zhou, Effective random laser action in Rhodamine 6G solution with Al nanoparticles. Appl. Opt. **50**, 1816–1821 (2011)
9. L. Li, L. Deng, Low threshold and coherent random lasing from dye-doped cholesteric liquid crystals using oriented cells. Laser Phys. **23**, 085001 (2013)
10. R.A. Benjamin, R. Gunawidjaja, H. Eilers, Photodegradation and self-healing in a Rhodamine 6G dye and Y_2O_3 nanoparticle-doped polyurethane random laser. Appl. Phys. B **120**, 1–12 (2015)
11. K. Cyprych, L. Sznitko, O. Morawski, A. Miniewicz, I. Rau, J. Mysliwiec, Spontaneous crystalization and aggregation of DCNP pyrazoline-based organic dye as a way to tailor random lasers. J. Phys. D Appl. Phys. **48**, 195101 (2015)

12. L. Cerdán, A. Costela, G. Durán-Sampedro, I. García-Moreno, Random lasing from sulforhodamine dye-doped polymer films with high surface roughness. Appl. Phys. B **108**, 839–850 (2012)
13. L. Ye, C. Hou, C. Lv, C. Zhao, Z. Yin, Y. Cui, Y. Lu, Tailoring of random lasing characteristics in dye-doped nematic liquid crystals. Appl. Phys. B **115**, 303–309 (2014)
14. W.Z.W. Ismail, T.P. Vo, E.M. Goldys, J.M. Dawes, Plasmonic enhancement of rhodamine dye random lasers. Laser Phys. **25**, 085001 (2015)
15. G.A. Kumar, N.V. Unnikrishnan, Energy transfer and optical gain studies of FDS:RhB dye mixture investigated under cw laser excitation. J. Photochem. Photobiol., A **144**, 107–117 (2001)
16. B.W. van der Meer, G. Coker, S.Y. Chen, Resonance Energy Transfer: Theory and Data (Wiley, New York, 1994), p. 177
17. D.L. Andrews, A unified theory of radiative and radiotionless molecular energy transfer. Chem. Phys. **135**, 195–201 (1989)
18. S. Xiaoyu, Y. Wang, Z. Wang, S. Wei, Y. Sun, D. Liu, J. Zhou, Y. Zhang, J. Shi, Random lasing with a high quality factor over the whole visible range based on cascade energy transfer. Adv. Opt. Mater. **2**, 88–93 (2013)
19. L. Cerdán, E. Enciso, V. Martín, J. Bañuelos, I. López-Arbeloa, A. Costela, I. García-Moreno, FRET assisted laser emission in colloidal suspensions of dye-doped latex nanoparticles. Nat. Photonics **6**, 621–626 (2012)
20. K.S. Alee, S. Barik, S. Mujumdar, Forster energy transfer induced random lasing at unconventional excitation wavelengths induced random lasing at unconventional excitation wavelengths. Appl. Phys. Lett. **103**, 221112 (2013)
21. J.F. Galisteo-López, M. Ibisate, C. Lopez, FRET-tuned resonant random lasing. J. Phys. Chem. C **118**, 9665–9669 (2014)
22. M.A. Ali, S.A. Ahmed, Comprehensive examination of radiationless energy transfer models in dyes: comparisons of theory and experiment. J. Chem. Phys. **90**, 1484–1491 (1989)
23. C. Lin, A. Dienes, Study of excitation transfer in laser dye mixtures by direct measurement of fluorescence lifetime. J. Appl. Phys. **44**, 5050–5052 (1973)
24. J.R. Lackowicz, *Principles of fluorescence* (Springer, New York, 1999)
25. W. Brown, K. Mortensen, *Scattering in polymeric and colloidal systems* (Gordon and Breach Science Publishers, Amsterdam, 2000)
26. M.P. Van Albada, A. Lagendijk, Observation of weak localization of light in a random medium. Phys. Rev. Lett. **55**, 2692–2695 (1985)
27. H. Cao, Lasing in random media. Waves Random Media **13**, R1–R39 (2003)
28. J.P. Tardivo, A.D. Giglio, C.S. de Oliveira, D.S. Gabrielli, H.C. Junqueira, D.B. Tada, D. Severino, R.D.F. Turchiello, M.S. Baptista, Methylene blue in photodynamic therapy: from basic mechanisms to clinical applications. Photodiagn. Photodyn. Therapy **2**, 175–191 (2005)
29. R.F. Kubin, A.N. Fletcher, Fluorescence quantum yields of some rhodamine dyes. J. Lumin. **27**, 455–462 (1983)
30. A. Penzkofer, Y. Lu, Fluorescence quenching of Rhodamine 6G in methanol at high concentration. Chem. Phys. **103**, 399–405 (1986)
31. R. Ghazya, S.A. Zimb, M. Shaheena, F. El-Mekaweya, Experimental investigations on energy-transfer characteristics and performance of some laser dye mixtures. Opt. Laser Technol. **34**, 99–105 (2002)